Biochimica et Biophysica Acta 1823 (2012) 2–14

Contents lists available at ScienceDirect

Biochimica et Biophysica Acta

journal homepage: www.elsevier.com/locate/bbamcr

Review

Structure and function of the AAA+ nucleotide binding pocket ☆

Petra Wendler *, Susanne Ciniawsky, Malte Kock, Sebastian Kube

Gene Center, Ludwig-Maximilians-Universität München, Feodor Lynen Strasse 25, 81377 München, Germany

ARTICLE INFO

Article history:
Received 2 May 2011
Received in revised form 17 June 2011
Accepted 27 June 2011
Available online 28 July 2011

Keywords:
AAA+ ATPases
Nucleotide binding pocket
Structural analysis
Functional analysis

ABSTRACT

Members of the diverse superfamily of AAA+ proteins are molecular machines responsible for a wide range of essential cellular processes. In this review we summarise structural and functional data surrounding the nucleotide binding pocket of these versatile complexes. Protein Data Bank (PDB) structures of closely related AAA+ ATPase are overlaid and biologically relevant motifs are displayed. Interactions between protomers are illustrated on the basis of oligomeric structures of each AAA+ subgroup. The possible role of conserved motifs in the nucleotide binding pocket is assessed with regard to ATP binding and hydrolysis, oligomerisation and inter-subunit communication. Our comparison indicates that in particular the roles of the arginine finger and sensor 2 residues differ subtly between AAA+ subgroups, potentially providing a means for functional diversification. This article is part of a Special Issue entitled: AAA ATPases: structure and function.

1. Many AAA+ proteins are p-loop containing molecular motors

A large range of molecular motors use the energy of ATP binding and hydrolysis to perform mechanical work. Included in this group are the dynein, myosin and kinesin superfamilies and a heterogeneous collection of ASCE (*a*dditional *s*trand *c*onserved *E* family; formerly RecA like) proteins, such as the AAA+ superfamily (extended *A*TPases *a*ssociated with various cellular *a*ctivities), the ABC (*A*TP *b*inding *c*assette) superfamily and helicase superfamilies I, II and III. The unifying structural motif shared by all these ATPases and some related GTPases is the p-loop (phosphate loop; [1]), which coordinates the β and γ phosphates of the nucleotide during hydrolysis. Yet, there is no overall sequence similarity between members of the superfamilies and their biological functions are very diverse as they range from actin and microtubule based motility to fusion of and transport across membranes, chromatin maintenance, coordinated proteolysis and disaggregation. Substrates of the ATPases are either oligonucleotides or proteins, which are moved relative to the stationary enzyme or are used to move the enzyme along a path. In general, interconnected dimers or oligomeric assemblies rather than just one ATPase domain perform the task. Whilst kinesin and myosin form a dimer of more or less indirectly interacting heads (reviewed in [2]), many ASCE proteins operate by direct interaction of several nucleotide binding domains. These multiple ATPase domains can either be on the same or different polypeptide chains. Examples of proteins that act as a dimer of two covalently linked ASCE domains are UvrD, PcrA and RecB in helicase superfamily I, RecG, eIF4A and NS3 in helicase superfamily II (reviewed in [3] and [4]) and the ABCA and ABCC subfamilies of the ABC ATPases [5]. In the case of the dynein and Rea1/midasin motor domains six ASCE domains are arrayed in one polypeptide chain, forming a hexameric ring of active and inactive ATPase domains [6,7]. However, many ASCE proteins function as homo- or heterooligomers. These motor complexes can be composed of two proteins such as the ABCD and ABCG subfamilies of the ABC ATPases [5], five proteins such as the clamp loaders [8], six proteins such as most classical AAA proteins [9] or seven proteins such as the *Aquifex aeolicus* NtrC1 σ^{54} activator [10]. In addition, hexameric motor complexes like Clp/Hsp100 proteins, p97 or NSF assemble as protomers of two covalently linked ASCE domains, bringing together 12 ATPase domains to form one active protein complex. In this review we focus on the hexameric AAA+ proteins and analyse the structures in the PDB with regard to conserved nucleotide binding motifs and oligomer contacts. We also provide a summary of relevant mutational analyses, without claiming a complete coverage of the available biochemical data. A good survey and visualisation of the evolutionary classification of ASCE proteins can be found elsewhere [11–13].

2. Classification of AAA+ ATPases

The first suggestion that ATPases of different functions but similar peptide sequence group into a novel family of AAA proteins was published in 1991 [9]. At that time the family comprised four members. Over the past 20 years, at least 30.000 AAA+ proteins have been identified throughout all kingdoms of life (Pfam ID:

Abbreviations: aa, *Aquifex aeolicus*; af, *Archeoglobus fulgidus*; ap, *Aeropyrum pernix*; av, Adeno-associated virus-2; bs, *Bacillus subtilis*; cg, *Ceanothus griseus*; ec, *Escherichia coli*; hs, *Homo sapiens*; LTag, large T-antigen; mj, *Methanocaldococcus jannaschii*; mm, *Mus musculus*; pa, *Pyrobaculum aerophilum*; pf, *Pyrococcus furiosus*; rn, *Rattus norvegicus*; sc, *Saccharomyces cerevisiae*; st, *Salmonella typhimurium*; SV, Simian virus; ta, *Thermoplasma acidophilum*; tm, *Thermotoga maritima*; to, *Thermococcus onnurieneus*; tt, *Thermus thermophilus*

☆ This article is part of a Special Issue entitled: AAA ATPases: structure and function.

* Corresponding author.
E-mail address: wendler@genzentrum.lmu.de (P. Wendler).

0167-4889/$ – see front matter © 2011 Elsevier B.V. All rights reserved.
doi:10.1016/j.bbamcr.2011.06.014

PF00004; Interpro ID: IPR003959) with eukaryotic genomes typically encoding 50–100 different proteins of this superfamily (supfam.org; [14]). The divergent appearance of the superfamily and the ambiguous boundaries to other p-loop NTPases complicates classification into defined subgroups. However, with a growing number of sequences, structures and biochemical studies available, unifying and divergent features of AAA+ ATPases become more apparent. Classifications comprising sequence alignments and morphological traits suggest that the primary characteristic features of AAA+ proteins are the presence of a conserved ASCE core domain and an additional α-helical, C-terminal domain (Fig. 1A; [11,13]). Further subclassification based on the topology of the AAA+ domain or the C-terminal domain identified several higher-order groups or clades. At the core of the superfamily are the classic AAA ATPases (classical AAA clade or extended AAA group), including the NSF, CDC48, Pex, Bcs, proteasomal ATPase, katanin, Vps4, FtsH, Tip49 and Clp Domain 1 (D1) families with the latter three families diverging from the others. A potpourri of **p**rote**a**ses, **c**helatases, **t**ranscriptional activators and **t**ransport proteins, named PACTT or Pre-sensor I insert superclade, forms another major subgroup within the AAA+ ATPases. It includes the σ^{54} activator, Lon A, MCM, MoxR, midasin, dynein and Mg-chelatase families at its core and the peripherally connected HslU, ClpX, Clp D2 and Lon B families. A third group is formed by **hel**icases and **c**lamp loaders (HEC group or clamp loader clade) such as the RuvB, RFC and γ/δ′-Pol III families. However, the classification for some AAA+ families has not been conclusively determined. Proteins involved in replication initiation for example establish an independent lineage (DnaA, CDC6, ORC clade) in the classification of Iyer et al. [11] but are included in the HEC group in the study of Ammelburg et al. [13]. Ammelburg et al. also identified the **s**ignal **t**ransduction **A**TPases with **n**umerous **d**omains (STAND) family and the ExeA family as independent subfamilies of the AAA+ proteins and excluded the helicase III superfamily on the basis of an aberrant topology of the C-terminal domain. In this review we mainly discuss members of the classical AAA ATPase group, the PACTT group and the HEC group, but also refer to some superfamily III helicases.

3. The nucleotide binding domain of AAA+ ATPases

The defining feature of all AAA+ proteins is a ~230 amino acid ATPase module, composed of the nucleotide binding ASCE and the α-helical, C-terminal subdomains (Fig. 1). The ASCE core structure is characterised by the 51432 order of the central, parallel β-sheet and the presence of two acidic residues in the Walker B motif. The Walker A (p-loop) and Walker B motifs are located at the tip of β strands 1 and 3, respectively. They are crucially involved in nucleotide binding and hydrolysis by coordinating the β and γ phosphates of ATP and the water activating magnesium ion [15]. In contrast to other NTPases the two Walker motifs in ASCE ATPases are separated by the β4 strand insertion. The tip of this strand typically carries a polar residue in the sensor 1 motif that participates in hydrolysis by coordinating the attacking water in concert with the Walker B residues. Depending on the topology of each AAA+ subfamily, the substrate interacting loops are located in insertions in the α2 helix and/or the α3 helix (reviewed in [12]). In the oligomeric complex the loops are typically oriented towards the central pore of the ring shaped assembly. An analysis of side chain conformations in 50 AAA+ crystal structures showed that the conserved glutamate in the Walker B motif of most AAA+ ATPases can switch from an active to an inactive conformation upon ATP binding (glutamate switch; [16]). In the inactive, ATP bound state the glutamate interacts with a conserved asparagine on the β2 strand and is only released into the fully active ATPase configuration by substrate binding. This model provides a means to link ATP hydrolysis with substrate interaction and would explain why some ATPases are only

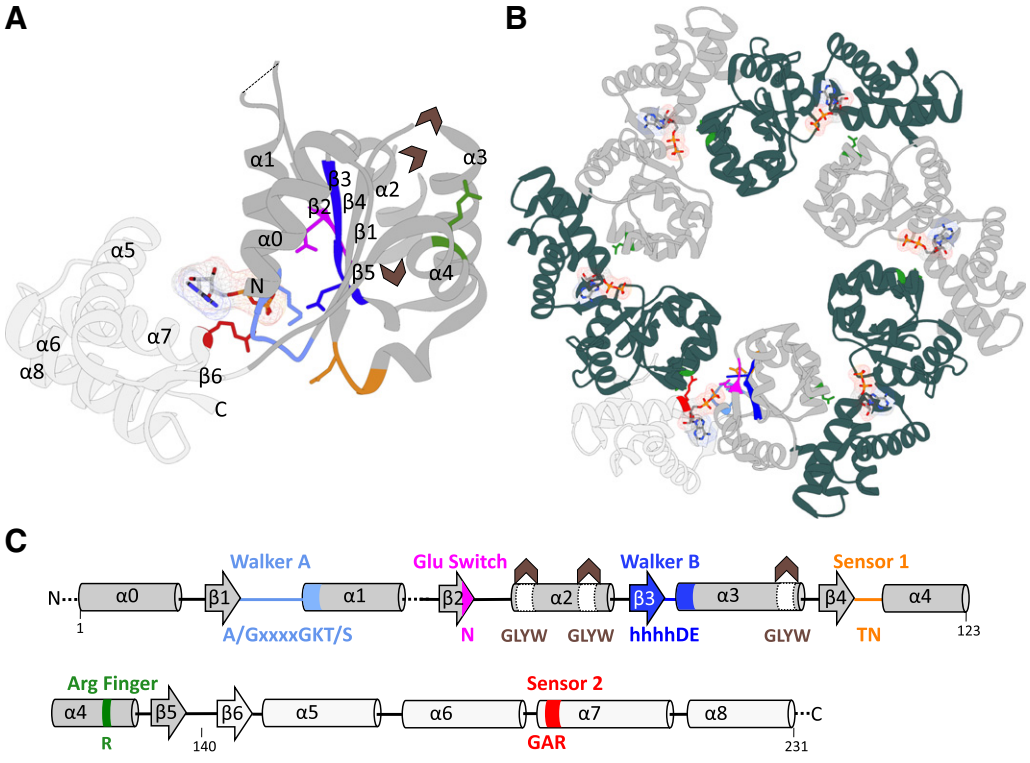

Fig. 1. Structure and oligomeric arrangement of the AAA+ domain. The AAA+ ATPase module (A) and its hexameric assembly (B) as seen in many crystal structures are depicted using the example of *to*Lon bound to ADP (PDB ID: 3K1J). Only the core ATPase domains of *to*Lon are shown. In (A) the ASCE domain is coloured in dark grey and the C-terminal domain in light grey. All structural elements are highlighted according to the colour code in the secondary structure annotation (C). Consensus sequences for each motif are given. Brown arrows indicate the position of pore loop insertions present in different AAA+ subgroups. Visible secondary structural elements are numbered in the order of appearance from N- to C-terminus. Protomers of the hexameric assembly in (B) are coloured alternating in dark green and grey. One protomer is coloured as shown in (A). Arginine fingers are coloured in green and the nucleotide is shown as stick and surface representation in all protomers.

Table 1
Summary of functional studies on AAA+ proteins. Effects of site directed mutagenesis on oligomerisation and enzymatic activity of selected AAA+ proteins are listed. The assembly state is denoted by numbers of associating monomers in the absence (−) or presence of ATPγS (G), ADP (D) or ATP (T). *In vitro* (solid colour), *in vivo* (striped) and basal NTPase activities are expressed as percentage of wild-type (see colour scale) [81-122].

	Mutation	Assembly	Activity	NTPase	Ref.	
*ec*ClpA	K220R	6^T			[81]	Walker A
	K220Q	$1^T, 2^T$			[81]	
	K501R/Q	6^T			[81]	
	K220Q/K501Q	6^T			[81]	
*ec*ClpB	K212A	$1^T, 2^T$			[47]	
	K611A	6^T			[47]	
	K212A/K611A	$1^T, 2^T$			[47]	
	K212T	$1^T, 1^-, 2^T, 2^-$			[89]	
	K611T	6^T			[89]	
	K212T/K611T	$1^T, 1^-, 2^T, 2^-$			[89]	
	K212T	$6^T, 6^-$			[95]	
	K611T	$6^T, 6^-$			[95]	
	K212T/K611T	$6^T, 6^-$			[95]	
*tt*ClpB	K204Q	6^T			[22]	
	K601Q	6^T			[22]	
	K204Q/K601Q	$<6^T, <6^D$			[79]	
	K204A/T205A	$<6^T$			[46]	
	K601A/T602A	6^T			[46]	
	K204A/T205A/ K601A/T602A	6^T			[46]	
*bs*ClpC	K214Q				[106]	
	K551Q				[106]	
	K214Q	$2^T, 6^T$			[37]	
	K551Q	$2^T, 6^T$			[37]	
	K214Q/K551Q	6^T			[37]	
*ec*ClpX	K124Q				[35]	
*sc*Hsp104	K218T	$6^D, 6^G$			[107,45]	
	K620T	$6^D, 6^G$			[107,45]	
	K218T	$1^-, 2^-, 6^T$			[108,109]	
	K620T	$1^T, 2^T, 1^-, 2^-$			[108,109]	
	K620T	6^T			[110]	
	K218T	6^T			[29]	
	G217V	6^T			[29]	
	K620T	1^T			[29]	
	G619V	1^T			[29]	
*sc*Hsp78	K149T	$6^T, 1^-, 2^-$			[111]	
	K547T	$1^T, 2^T, 1^-, 2^-$			[111]	
	K149T/K547T	$1^T, 2^T, 1^-, 2^-$			[111]	
*rn*p97/VCP	K251A	6			[113]	
	K524A	6			[113]	
	K251A/K524A	6			[113]	
*mm*p97/VCP	K251A	1, 6			[71]	
	K524A	6			[71]	
*hs*p97/VCP	K251T	$1^T, 1^-, 6^T, 6^-$			[26,116]	
	K524T	$1^-, 6^-, 6^T$			[26,116]	
	K251T/K524T	$1^-, 6^-$			[26,116]	
*ta*p97/VAT	K237A	6^T			[44]	
	K514A	6^T			[44]	
	K237A/K514A	6^T			[44]	
*ec*FtsH	K201N				[58]	
	K198N				[118]	
*ec*HslU	K63T	$1^T, 1^D$			[120]	
*ec*RuvB	K68A	6^T			[121]	
	K68R	$6^T, 12^T$			[121]	
	T69A	6^T			[121]	

	Mutation	Assembly	Activity	NTPase	Ref.	
*ec*RuvB	T69S				[82]	Walker A
	K68R				[82]	
*hs*NSF	K266A				[23]	
	K549A				[23]	
*sc*Vps4	K179A	2^D			[83,40]	
*hs*Vps4	K173Q (4A)				[41]	
	K180Q (4B)				[41,85]	
SV40 LTag	G431ALE	1^T			[90]	
	D429S/S430R				[91]	
*st*NtrC	G173N				[93]	
*hs*Ras/GAP	G12A/R (Ras)	Ras-RasGAP			[17,96]	
	G12P (Ras)	Ras-RasGAP			[17,96]	
	G12L/I/V/D (Ras)	Ras-RasGAP			[17,96]	
*ta*Lon	K63A	6^-			[92]	
*sc*CDC6	K114E/P				[102,97]	
	K114Q/L				[102]	
	K114A				[97]	
	K114R				[102]	
*hs*RFC	K84A (p37)	5^-			[105]	
	K66A (p36)	5^-			[105]	
	K82A (p40)	5^-			[105]	
*af*RFC	K49D/T50D (L)	5			[99]	
	K51D/T52D (S)	5			[99]	
	K49D/T50D (L)/ K51D/T52D (S)	5			[99]	
*mj*PAN	K217R				[103]	
*ec*ClpA	E286A	6			[43]	Walker B
	E565A	6			[43]	
	E286A/E565A	6			[43]	
*ec*ClpB	E279A	6^T			[47]	
	E678A	6^T			[47]	
	E279A/E678A	6^T			[47]	
*tt*ClpB	E271A/E668A	$6^T, <6^D$			[79]	
	D270N	6^T			[46]	
	E271Q	6^T			[46]	
	D667N	6^T			[46]	
	E668Q	6^T			[46]	
*bs*ClpC	E280A	6^T			[37]	
	E618A	6^T			[37]	
	E280A/E618A	6^T			[37]	
*ec*ClpX	E185Q	6^T			[114]	
*sc*Hsp104	E285Q				[45]	
	E687Q				[45]	
	E285Q/E687Q	$6^T, 6^D, 6^G$			[45,107]	
*mm*p97/VCP	E305Q				[71]	
	E578Q				[71]	
*hs*p97/VCP	E305Q				[116]	
	E578Q				[116]	
	E305Q/E578Q	$1^-, 6^-, 6^T$			[26,116]	
*ta*p97/VAT	E291A	6^T			[44]	
	E568A	6^T			[44]	
	E291A/E568A	6^T			[44]	
*ec*RuvB	D113G				[82]	
	H116Y/R				[82]	
*hs*NSF	E329Q				[23]	

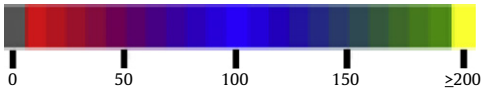

Table 1 (*continued*)

	Mutation	Assembly	Activity	NTPase	Ref.	
*hs*NSF	E329Q/D604Q				[23]	Walker B
	D604Q				[23]	
*sc*Vps4	E233Q	2^D, 8^T, 10^T			[83,40,84]	
*hs*Vps4	E228Q (4A)				[41]	
	E235Q (4B)				[41,85]	
SV40 LTag	D474N/A	6^T, 1^-			[86,87]	
	E473A/D474A				[88]	
*st*NtrC	D239A/C/N				[61]	
*ta*Lon	D241A	6^-			[92]	
*sc*CDC6	E224G				[94]	
	D223A/E224A				[97]	
*af*RFC	E112A (L)	5			[99]	
	E110A (S)	5			[99]	
*mj*PAN	E271K				[100]	
	E271Q				[103]	
*hs*Ras/GAP	Q61A (Ras)				[96]	S witch 2
	Q61N/L (Ras)				[96]	
*sc*Hsp104	T317A	6			[21]	Sensor 1
	N728A	6			[21]	
*hs*p97/VCP	N348Q				[59]	
*ta*p97/VAT	N334A	6^T			[44]	
	N612A	6^T			[44]	
	N334A/N612A	6^T			[44]	
*ec*FtsH	D307E				[58]	
	D307N				[58]	
*ec*RuvB	G159A				[82]	
	G159R				[82]	
	A160G				[82]	
	A160R				[82]	
	T161A				[82]	
	T161S				[82]	
	T162A				[82]	
*tm*RuvB	A156S				[60]	
	A156C				[60]	
	T157V/T158V				[60]	
	T158V				[60]	
*hs*NSF	T373A	6^T			[38]	
	N374A	6^T			[38]	
	N374D	6^T			[38]	
	R375A	6^T			[38]	
	R375E	6^T			[38]	
SV40 LTag	N529A	1^T, 1^-, 6^T, 6^-			[87]	
*ta*Lon	N293A	6^-			[92]	
*sc*CDC6	N263A				[101,104]	
	N263D				[104]	
*ec*ClpB	G813A/R815A	6^T			[47]	Sensor 2
*ec*ClpX	R370K	6^T			[57]	
*sc*Hsp104	R826M	6			[119]	
*ec*HslU	R393A	1^T, 6^T			[112]	
*ec*RuvB	T219A				[82]	
	R221A				[82]	
	R225A				[82]	

	Mutation	Assembly	Activity	NTPase	Ref.	
*ec*RuvB	R228A				[82]	Sensor 2
	R229A				[82]	
*tm*RuvB	P216G				[60]	
	R217K				[60]	
	R217A				[60]	
*hs*NSF	E440A	6^T			[38]	
	E440R	6^T			[38]	
	L441A	6^T			[38]	
	E442A	6^T			[38]	
	E442R	6^T			[38]	
*st*NtrC	R358C/H				[98,61]	
*ta*Lon	R375A	6^-			[92]	
	R382A	6^-			[92]	
*sc*CDC6	D330A				[101]	
	D330N				[101]	
	R332A/E				[101,104]	
*ec*ClpB	R332A	1^T, 6^T			[47]	Arginine Finger
	R756A	6^T			[47]	
*bs*ClpC	R332A	2^T			[37]	
*sc*Hsp104	R334M	1^T, 6^T			[72]	
	R765M	6^T, 6^-			[72]	
*hs*p97/VCP	R359E	6			[59]	
	R362E	1, 3, 6			[59]	
	R359K	6			[59]	
	R635A/K	6			[59]	
	R638A/K	6			[59]	
	R359E/R362E	1, 3, 6			[59]	
	R635E/R638E	6			[59]	
	R359A	6			[59]	
	R362A	6			[59]	
	R362K	6			[59]	
	R359A/R362A	6			[59]	
	R635A/R638A	6			[59]	
*ec*FtsH	R312L				[58]	
	R312K				[58]	
	R315L				[58]	
	R315K				[58]	
*ec*HslU	R325E	1^T			[112]	
*ec*RuvB	R174H				[82]	
*tm*RuvB	R170A/K				[60]	
*hs*NSF	R388A	6^T			[38]	
	R385A	6^T			[38]	
	R385A				[115]	
	R388A				[115]	
SV40 LTag	R540A	1^T, 1^-, 6^T, 6^-			[87]	
*st*NtrC	R294C	7			[98,61]	
*hs*Ras/GAP	R789A/K (GAP)	Ras-RasGAP			[18]	
*ta*Lon	R305A	6^-			[92]	
*sc*RFC	R157Q (B)				[117]	
	R160Q (C)				[117]	
	R183Q (D)				[117]	
	R184Q (E)				[117]	
*ec*Clamp Loader	R169A (γ)	5^T			[122]	

fully active when co-factors and substrate are bound. Another defining feature of AAA+ ATPases is the presence of one or more arginine residues at the end of helix α4. In the active oligomer, these residues are located in proximity to the γ phosphate of the bound ATP in the neighbouring subunit. They are often termed arginine fingers, referring to the resembling arrangement of the nucleotide binding

pocket found in small GTPases [17]. There, the GTPase activity is enhanced by up to five orders of magnitude through interaction with its GAP (*G*TPase *a*ctivating *p*rotein), which provides an arginine to stabilise the transition state during GTP hydrolysis. However, not all GTPases follow this principle. The activating proteins of the Ran and Rap GTPases lack an arginine finger and Gα proteins carry an arginine finger on their integral α-helical domain insertion (reviewed in [18]). The C-terminal, α-helical subdomain of AAA+ proteins also harbours a well-conserved arginine residue. The so called sensor 2 motif is positioned at the tip of helix α7 and contacts the bound nucleotide [13,19]. It should be noted that the arginine finger, sensor 1 and sensor 2 residues are not conserved in all members of the AAA+ superfamily. Some of the DnaA, CDC6, ORC clade members, HslU, ClpX and the NSF D2 domain lack a functional sensor 1 and/or arginine finger residue. The classical AAA ATPases lack a sensor 2 residue.

3.1. Functional conservation of residues at the nucleotide binding pocket

In order to gain an overview of the functional conservation of the AAA+ motifs, we assembled biochemical data summarising the effects of mutations with regard to oligomerisation, basal hydrolytic NTPase activity and *in vivo* or *in vitro* activity (Table 1). For comparison we included mutations for at least one member of each AAA+ subgroup, a member of the helicase superfamily III (SV40 LTag helicase) and the Ras/p120GAP pair.

Given the conservation of the ATPase binding motif in AAA+ proteins, it is not surprising that most ATP interacting residues are essential for complex activity and do not tolerate even conservative amino acid exchanges. The most commonly mutated residue in the Walker A motif is the invariant lysine, which interacts with the β and γ phosphates of ATP and structures the p-loop in related NTPases [20]. Exchange to a polar amino acid typically abolishes ATP binding and therefore ATPase and *in vitro* activity of the complex. Furthermore, it frequently leads to dissociation of the hexameric assembly in single domain AAA+ ATPases, as seen for HslU and SV40 LTag helicase. Tandem domain ATPases like Clp/Hsp100, NSF and p97 usually show co-operativity and division of labour between the two domains [21–25]. One domain is responsible for oligomerisation whilst the second site displays elevated hydrolysis rates. Walker A mutations in individual domains can indicate their role in oligomerisation. ClpA and B hexamer formation are disturbed by Walker A lysine mutations in the D1 domain, whereas assembly of NSF, Hsp104 and Hsp78 is disrupted by equivalent mutations in the D2 domain. For p97/VCP it has been shown that the D1 domain is important for oligomerisation and is most likely irreversibly bound to ADP during hexamer formation [26–28]. Interestingly, hexamer stability in these proteins is not only dependent on nucleotide binding, but also on the ionic strength of the buffer. Whilst p97/VCP hexamers withstand up to 6 M urea [26], ClpB/Hsp104 hexamers start to dissociate when salt concentrations exceed 50 mM [22,29,30]. ClpB/Hsp104 proteins can also oligomerise under low salt conditions (20–50 mM salt) without nucleotide present, whereas p97, ClpA, ClpX, ClpC and NSF are routinely assayed in the presence of ATP and 100–300 mM salt [31–39]. On the other hand *sc*Vps4 does not form higher oligomers *in vitro* unless the protein carries a Walker B mutation and ATP is present [40,41]. At this point it should be noted that the biochemical results summarised in Table 1 might differ for identical mutations. This is most likely due to different experimental set up, such as ionic strength of the buffer, nucleotide and/or protein concentrations.

The most common mutations of the Walker B motif are amino acid exchanges of the conserved glutamate and aspartate residues to glutamine or alanine. The negatively charged residues prime a water molecule for a nucleophilic attack on the γ phosphate group of ATP [42] and when mutated ATP hydrolysis but not ATP binding is abolished. All single domain AAA+ proteins show 80%–100% activity loss *in vitro* and *in vivo* despite forming stable oligomers. In tandem domain Clp ATPases and NSF a Walker B mutation in the module responsible for oligomerisation barely alter the ATPase activity of the complex. In some cases (ClpA, p97) this mutation does not even influence substrate degradation *in vitro* [43,44]. Interestingly, Walker B mutations in the site of high hydrolytic activity in ClpB (D2) and Hsp104 (D1) stimulate ATP hydrolysis in the other AAA+ domain to 4- to 10-fold wt activity, indicating intra subunit co-operativity [45–48].

Several crystal structures of ASCE ATPases show that polar residues in the sensor 1 motif are part of a hydrogen-bonding network that positions the attacking water molecule relative to the γ phosphate of ATP [49–51]. This led to the suggestion that these residues act as sensors to mediate conformational changes in analogy to the switch II region in the structure of Ras [52]. Hattendorf and Lindquist demonstrated that mutations of Hsp104 sensor 1 residues threonine (D1) and asparagine (D2) to alanine dramatically reduce ATP turnover rates *in vitro* and result in a loss of function *in vivo*, arguing that sensor 1 residues participate in nucleotide hydrolysis rather than sensing [21]. Indeed, similarly to Walker B mutations, most sensor 1 mutations dramatically impair ATP hydrolysis and complex activity *in vivo* or *in vitro* despite efficient oligomerisation (Table 1). The movement of the sensor 1 residue upon engagement with the nucleotide in the binding pocket of p97 D2 is thought to be transmitted through the central β sheet causing displacements of up to 3 Å at the distal end of the ASCE domain, where the arginine fingers are located [53]. However, mutation of this sensor 1 residue in the archeal p97 variant VAT has no effect on ATPase activity *in vitro* [44] suggesting that the signal transduction cascade is not essential for activity or that the homologues show functional differences. Not all AAA+ proteins posses a polar residue in the sensor 1 position. In the Orc2 family, some CDC6/Orc1 proteins, ClpX and HslU an alanine or histidine residue is located at this position [11,54] and there is so far no indication that these amino acids are involved in ATP hydrolysis.

The conserved arginine in the α-helical subdomain was termed sensor 2 residue in analogy to arginines in a subdomain of adenylate kinase, which contact the phosphate groups of ATP and mediate a conformational change that sequesters the catalytic site from water [55]. Indeed, in most AAA+ crystal structures this residue interacts directly with the β and γ phosphates of ATP (Fig. 2). Mutations of the sensor 2 residue lead to a loss or decrease of ATP binding as seen for NtrC1 and Hsp104 and/or severe defects in ATP hydrolysis as seen for HslU, ClpX and RuvB (reviewed in [56]). Although the sensor 2 residue has been implicated with protomer communication by mediating conformational changes of the C-terminal domain [57], mutations at this position do not impair hexamerisation. Members of the extended AAA ATPases have no sensor 2 residue. Interestingly, the Clp/Hsp100 D1 subgroup posses a highly conserved arginine residue, which is located 4 amino acids upstream the sensor 2 position (Fig. 2A).

The arginine finger residues of AAA+ proteins have been studied extensively (Table 1). Even conservative mutations often result in a complete loss of *in vivo* and/or *in vitro* activity of the complex [58–60], indicating that these residues are necessary for ATP hydrolysis. They also seem to be important for hexamer stability, since arginine finger mutations in HslU, p97 VCP, ClpB D1, ClpC D1 and Hsp104 D1 impair oligomer formation even in the presence of ATP (Table 1). In this regard AAA+ protein arginine finger mutations clearly differ from Ras/RasGAP arginine finger mutations, which do not interfere with complex formation. Altogether, arginine finger mutations in AAA+ proteins have a similar phenotype as Walker A mutations, suggesting that arginine fingers might also participate in nucleotide binding. Studies on NtrC1 and FtsH however clarified that the arginine finger residues are not involved in ATP binding [58,61]. More recently, a bottom-up study on isolated ClpB D2 domains also demonstrated that dimer formation and thus arginine finger contacts are not required for nucleotide binding [62]. The destabilising effect of arginine finger

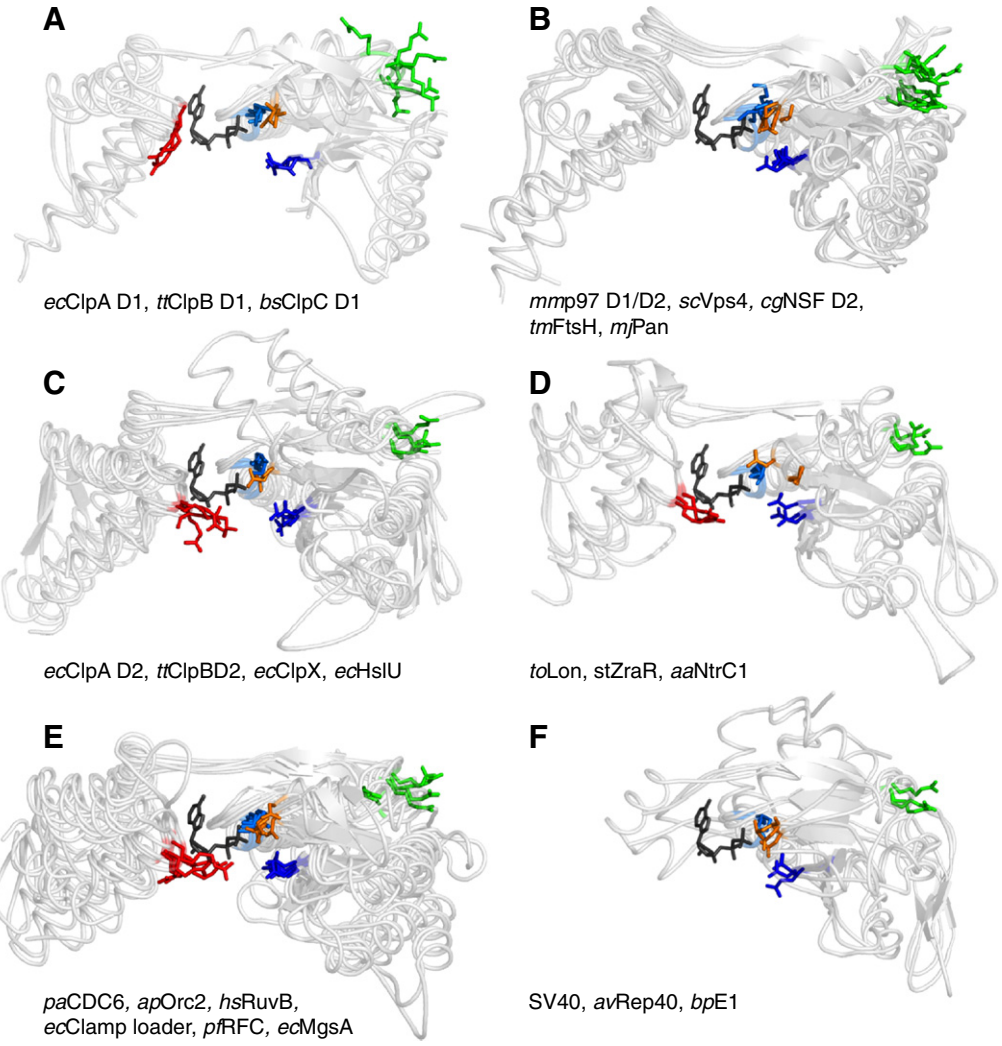

Fig. 2. Structural conservation of nucleotide interacting residues in AAA+ proteins. Global superposition of crystal structures of the classic AAA+ group- Hsp100 D1 (A) the extended AAA+ group (B), the PS I superclade (C), the PACTT core group (D), the HEC group (E) and helicase superfamily III (F) as listed in Table 2. Structures are superimposed on the ATP binding pocket using ClpB D1 (PDB ID: 1QVR; A, B), ClpB D2 (PDB ID: 1QVR; C, D), Orc2 (PDB ID: 1W5S; E) and SV40 (PDB ID: 1SVM; F) as reference structures. Conserved amino acid residues are shown as sticks and highlighted in cyan (Walker A), deep blue (Walker B), orange (sensor 1), green (arginine finger) and red (sensor 2). The highly conserved arginine residue close to the sensor 2 position in the Hsp100 D1 domains is also indicated in red (A). Nucleotides in the superposition derive from FtsH (PDB ID: 2CEA; A, B, C, D, E) and SV40 (PDB ID: 1SVM; F) and are depicted as dark grey stick models. Missing arginine residues in the structures of ClpC (PDB ID: 3PXI, R332/R333) and ClpX (PDB ID: 3HWS, R307) and asparagine residue of Rep40 (PDB ID: 1S9H, N421) were added using pymol (www.pymol.org). The UCSF Chimera [80] package was used for superposition of structures and images were generated in pymol.

mutations on the active AAA+ assembly remains puzzling. It is possible that the residues do not only participate in hydrolysis, but also account for subunit interface contacts or the structural integrity of the binding pocket.

3.2. Structural conservation of the nucleotide binding pocket

In order to visualise the similarities in the overall shape and size of the AAA+ core domain we grouped members of the superfamily according to recent classifications (Table 2) and overlaid AAA+ domains of available crystal structures of each member on their ATP binding pocket (Fig. 2). We did not incorporate the evolutionary more distant STAND and ExeA families, but included some helicase superfamily III ATPases for comparison. Important Walker A, Walker B, sensor 1, sensor 2 and arginine finger residues are displayed in the superposition.

The overall shape and dimensions of the AAA+ core domain are very similar in all proteins of the superfamily. Superposition of crystal structures of different AAA+ domains reveals the strong structural conservation of both subdomains. The ASCE fold is approximately $40 \times 40 \times 30$ Å, whereas the four-helix bundle of the C-terminal subdomain is roughly $30 \times 35 \times 25$ Å in size. It is not surprising that the spatial arrangement of the Walker A lysine, the Walker B aspartate and sensor 1 asparagine/threonine is very similar in all AAA+ proteins, given that all three residues are part of the hydrogen-bonding network surrounding the nucleotide. The position of the sensor 2 arginine is also maintained in all proteins of the PACTT and HEC groups (Fig. 2C, D, E). Members of the extended ATPase group lack an arginine in the α-helical subdomain (Fig. 2B), but usually possess two arginine finger residues spaced out over four amino acids. Exceptions to this rule are the Clp/Hsp100 D1 domains (Fig. 2A). They contain two consecutive arginine fingers, which are unevenly oriented in the crystal structures, forming the most divergent structural feature in the overlay. This group of AAA+ domains also displays a very conserved arginine residue close to the sensor 2 position that does not contact the nucleotide in the deposited crystal structures. The helicase superfamily III proteins possess an aberrantly

Table 2
Conserved nucleotide interacting residues of AAA+ proteins. List of structures used for the superposition in Fig. 2. The name and origin of the protein, the assembly state in the crystal, the PDB accession code, the nucleotide binding state and conserved amino acid residues highlighted in the superposition are given. Proteins are sorted according to the classification of Ammelburg et al. [13]. ClpX is a pseudohexamer of covalently linked trimers (*).

	Name	Assembly	PDB-ID	Nucleotide bound	Chain	Walker A	Walker B	Sensor I	Arginine finger	Sensor 2
Extended AAA group/classic clade	*ec*ClpA D1	Spiral	1R6B	ADP	X	K220	E286	T323	R339, R340	R392
	*tt*ClpB D1	Spiral	1QVR	ANP	A	K204	D270	T307	R322, R323	R375
	*bs*ClpC D1	Hexamer	3PXG	None	A	K214	D279	T316	R332, R333	R385
	*cg*NSF D2	Hexamer	1NSF	ATP	A	K549	D606	No	No	No
	*sc*Vps4	Monomer	3EIE	None	A	K179	D232	N277	R288,R289	No
	*mm*p97 D1	Hexamer	3CF1	ADP	A	K253	D304	N348	R359, R362	No
	*mm*p97 D2	Hexamer	3CF1	ADP-AlF3	A	K524	D577	N624	R635, R638	No
	*tm*FtsH	Hexamer	2CEA	ADP	A	K207	D260	N307	R318, R321	No
	*mj*Pan	Monomer	3H4M	ADP	A	K217	D270	T316	R328, R331	No
PACTT group/PS I superclade	*ec*ClpA D2	Spiral	1R6B	None	X	K501	D564	N606	R643	R702
	*tt*ClpB D2	Spiral	1QVR	None	A	K601	D667	N709	R747	R806
	*ec*ClpX	Hexamer*	3HWS	ADP	A	K125	D184	No	R307	R370
	*ec*HslU	Hexamer	1DO2	AMP PNP	A	K63	D256	No	R325	R393
PACTT core group	*to*Lon A	Hexamer	3K1J	ADP	A	K73	D245	N297	R311	R379
	*st*ZraR	Hexamer	1OJL	None	A	K175	D240	T281	R301	R359
	*aa*NtrC1	Heptamer	3M0E	ATP	A	K173	D238	N280	R299	R357
HEC group/DnaA Orc CDC6 clade	*pa*CDC6/Orc1	Monomer	1FNN	ADP	A	K57	D132	N168	R180	R241
	*ap*Orc2	Monomer	1W5S	ADP	A	K65	D145	No	No	R260
	*hs*RuvB	Hexamer	2C9O	ADP	A	K76	D302	N332	R357	R404
HEC group/clamp loader clade	*ec*Clamp loader	Pentamer	3GLF	ADP-AlF3	B	K51	D126	T157	R169	R215
	*pf*RFC	Hexamer	1IQP	ADP	A	K59	D117	N148	R160	R206
	*ec*MgsA	Tetramer	3PVS	None	A	K63	D113	T142	R156	R209
Helicase superfamily III	SV40 LTag helicase	Hexamer	1SVM	ATP	A	K432	E473	N529	R540	No
	*av*Rep40	Monomer	1S9H	None	A	K340	E378	N421	R444	No
	bpE1	Hexamer	2V9P	None	A	K439	D478	N523	R538	No

formed α-helical domain (Fig. 2F). For this reason they lack the sensor 2 arginine.

4. Interactions at the ATP binding pocket

Most hexameric AAA+ structures in the PDB show a typical domain arrangement in which the nucleotide binding pocket lies in the interface between two protomers. It is believed that in the active, ring shaped assembly the arginine finger of one subunit comes into close proximity to the nucleotide bound in the neighbouring subunit. In this state AAA+ ATPases show elevated ATPase activity, which can be abolished by mutations of the arginine finger. Based on this observation, it was suggested that the arginine finger contact stimulates ATPase activity in a similar manner as RasGAP activates Ras [58]. A closer look at the GTP binding site of the crystallised Ras/p120GAP/GDP AlF_3 complex reveals that the guanidine group of Arg^{789} is located 3.3 Å away from the β phosphate oxygen atoms of GDP (Fig. 3A). The closest distance between the fluoride groups of AlF_3 and the amino group of Arg^{789} amounts to 2.6 Å, allowing for interaction between the arginine finger and the nucleotide in its transition state.

The ATP binding pocket of the SV40 LTag helicase (helicase superfamily III) is formed by contribution of two positively charged residues from the neighbouring subunit, namely Arg^{540} and Lys^{418} (Fig. 3B). These residues are positioned 2.3–3.1 Å away from the ATPs γ phosphate and are part of an extensive hydrogen-bonding network. Interestingly, Lys^{418} rather than the conserved arginine finger residue Arg^{540} occupies the space that is taken by the arginine finger residue in the Ras/p120GAP pair.

Both AAA+ domains of p97 contain two conserved arginine finger residues and mutation of any of them leads to a complete or partial loss of ATPase activity (Table 1). At least 13 different hexameric crystal structures of p97 domains have been deposited in the PDB and the orientation of the arginine residues of some structures varies considerably, indicating side chain flexibility (reviewed in [56]). For our review we have chosen a crystal structure with close distances between arginine fingers and nucleotide in both binding pockets (PDB ID: 3CF1; Fig. 3C and D). A comparison of inter-atomic distances in different p97 structures is shown in Table 3. Until recently, only ADP bound forms of p97 D1 could be crystallised. In 2010 a disease associated, mutated D1 domain was crystallised in the presence of ATPγS and it could be demonstrated that ATP binding to this domain changes essential inter-domain interactions [28,63]. The hydrogen bond network around the p97 D1 nucleotide seems to include Arg^{359} but not Arg^{362}, which is 8.5 Å away from the ADP phosphate groups. This residue on the other hand interacts with the glutamic acid in the Walker B motif, possibly contributing to the overall organisation of the nucleotide binding pocket. A similar setup is observed in the p97 D2 domain. However, the distances between Arg^{635} and ADP AlF_3 or Walker B residues in the neighbouring subunit range from 4.7 Å to 5.2 Å and the residues are too far apart to allow for electrostatic interactions. In contrast to all preceding proteins, HslU contains a sensor 2 arginine that is located 2.8 Å away from the oxygen of the γ phosphate of ANP in the hexameric crystal structure (Fig. 3E). The predicted arginine finger residue Arg^{325} contacts neither the phosphates of the nucleotide (9.4 Å away) nor the Walker B glutamate residue, although there is a salt bridge between the Walker B glutamate and the non-conserved Arg^{279} of the neighbouring subunit. Intriguingly, the side chain orientations of all three residues are almost identical in superpositions of many HslU crystal structures (PDB ID: 1DO2, 1G41, 1DO0, 1E94, 1YYF, 1HQY) regardless of the nucleotide bound (Table 3). Notably, differences are seen in the ATP and HslV bound structure of HslU (PDB ID: 1G3I), where the sensor 2 side chain is rotated by ~7 Å, impacting on the orientation of the very C-terminal residues that connect HslU and HslV [64].

In NtrC1, also a member of the PACTT group, the sensor 2 and arginine finger residues are in very close proximity to the bound ATP in the crystal structure (Fig. 3F). The hydrogen-bonding network between protomers of this heptamer is maintained by electrostatic interactions within 2.9–4 Å and is reminiscent of the one in SV40 LTag hexamers and the clamp loader pentamers (Fig. 3B and G). It should be noted, that the NtrC1 structure carries an E239A Walker B

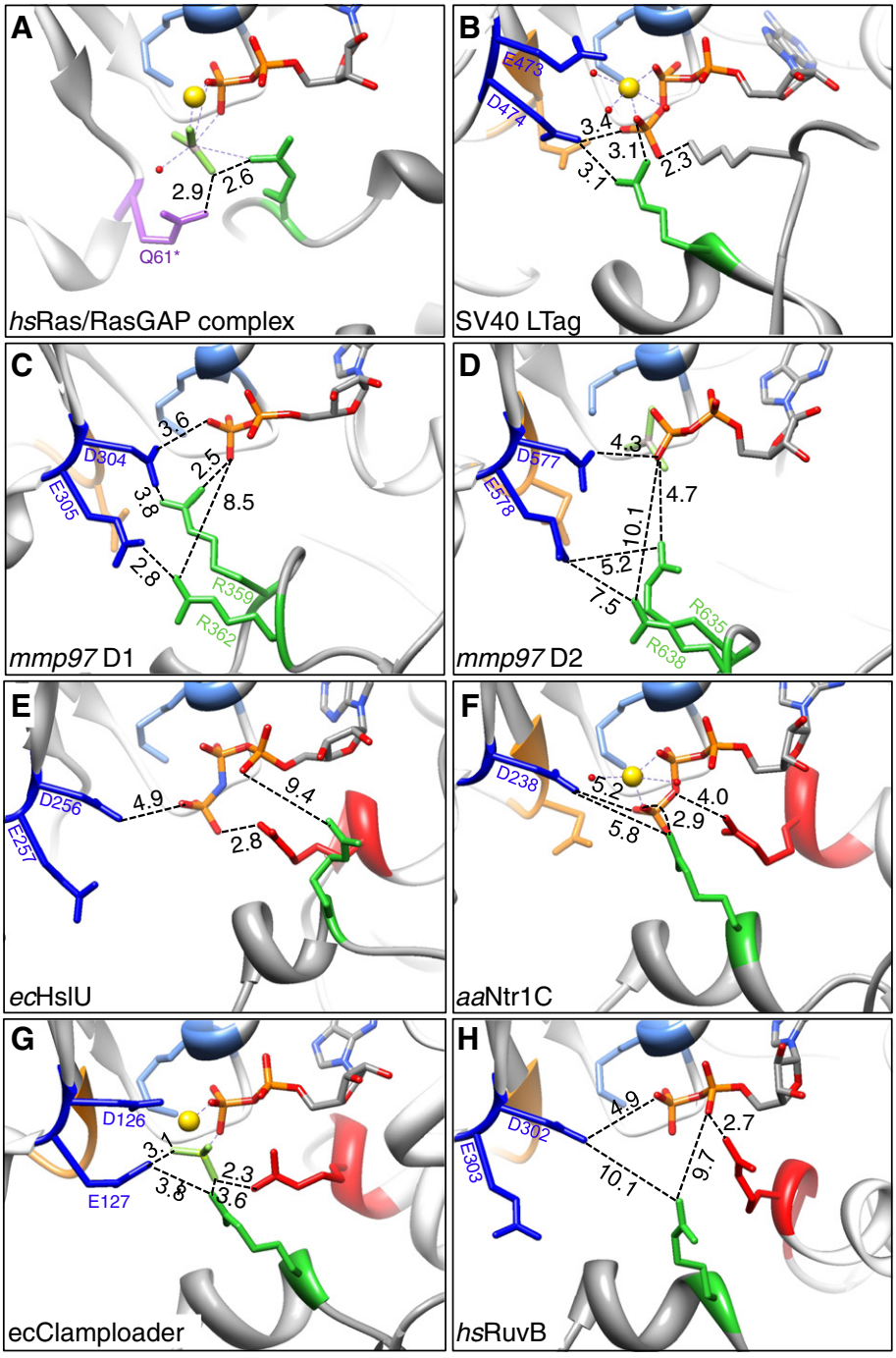

Fig. 3. ATP binding pockets of hexameric AAA+ crystal structures. Enlarged view of the nucleotide binding pocket of the *hs*Ras–p120GAP complex (A; PDB ID: 1WQ1), SV40 LTag helicase (B; PDB ID: 1SVM), *mm*p97 D1 (C; PDB ID: 3CF1), *mm*p97 D2 (D; PDB ID: 3CF1), *ec*HslU (E; PDB ID: 1DO2), *aa*NtrC1 (F; PDB ID: 3M0E), *ec*Clamp loader (G; PDB ID: 3GLF) and *hs*RuvB (H; PDB ID: 2C9O) protomers is displayed. All structures are overlaid on the p-loop region of the *hs*Ras–p120GAP complex using UCSF Chimera. Nucleotides, nucleotide analogues and important residues of the AAA+ domain are represented as stick models. The nucleotide is colour coded by elements and amino acids are coloured as shown in Fig. 1. The switch II region (Q61*) of the hsRas–p120GAP complex is depicted in purple. Distances are given in Å and represent the closest approach between the chosen residues.

mutation, which leads to a side chain rotation in the D238 Walker B residue and abolishes ATP hydrolysis. In the ADP AlF bound pentameric clamp loader complex the Walker B glutamate residue is interacting with the arginine finger and the AlF in the position of the γ phosphate. The sensor 2 and arginine finger residues come to lay 2.3 Å and 3.6 Å away from the AlF.

Finally, the structure of the human RuvB variant bound to ADP is surveyed as a second member of the HEC group of AAA+ proteins (Fig. 3H). The nucleotide binding site in this hexamer is mainly formed by residues from one protomer, since the arginine finger Arg^{357} is rotated away from the binding pocket. The distance between the sensor 2 arginine and the ADPs β phosphate is 2.7 Å and the distances between arginine finger and ADP or Walker B residues are ~10 Å.

It is noteworthy that the spatial arrangement of the conserved sensor 2 residue in crystal structures of all HEC and PACTT group proteins (Fig. 3E–H) is almost identical to the positioning of the arginine finger residue in Ras/p120GAP (Fig. 3A).

Table 3
Topological survey of the nucleotide binding site of oligomeric ASCE crystal structures. The closest approaches between atoms of the Walker B or arginine finger residues and the nucleotide and between both motifs in selected oligomeric ASCE crystal structures are listed. For distance measurements side chain carboxyl oxygen atoms of the Walker B residues, side chain amine nitrogen atoms of the arginine finger residue and oxygen atoms of the α, β or γ phosphate group of the nucleotide were used as indicated. The oligomeric state, PDB accession code, chain identifier and residues used for distance measurements for each structure are specified. ClpX is a pseudohexamer of covalently linked trimers (*). The structure of *bp*E1 was superimposed with the SV40 LTag helicase and the nucleotide bound to SV40 LTag helicase was used for distance measurements (**). All measurements were done using UCSF Chimera.

	Name	Oligomer	PDB-ID	Nucleotide bound	Chain	Walker B	Distance to nucleotide [Å]	Arginine finger	Distance to nucleotide [Å]	Closest inter-motif distance [Å]
Ras/p120GAP complex	*hs*Ras/p120GAP complex	Dimer	1WQ1	GDP-AlF3	R	N61	5.6^{β}	R789	3.3^{β}	5.0 (D57-R789)
Extended AAA group/classic clade	*cg*NSF D2	Hexamer	1NSF	ATP	A	D604	5.5^{γ}	None	–	–
	*mm*p97 D1	Hexamer	3CF1	ADP	B	D304	3.6^{β}	R359, R362	2.5^{β} (R359)	2.8 (E305-R362)
	*mm*p97 D1	Hexamer	3CF2	ADP	A	D304	4.5^{β}	R359, R362	2.9^{β} (R359)	2.2 (E305-R362)
	*mm*p97 D1	Hexamer	3HU1	ATPgS	A	E305	4.2^{γ}	R359, R362	6.2^{γ} (R359)	3.3 (E305-R362)
	*mm*p97 D2	Hexamer	3CF1	ADP-AlF3	B	D577	4.3^{β}	R635, R638	4.7^{β} (R635)	5.2 (E578-R635)
	*mm*p97 D2	Hexamer	3CF2	AMP-PNP	B	D577	3.1^{γ}	R635, R638	3.1^{γ} (R635)	2.3 (E578-R635)
	*tm*FtsH	Hexamer	2CEA	ADP	B	D260	4.7^{β}	R318, R321	10.9^{α} (R318)	5.9 (E261-R318)
PACTT group/PS I superclade	*ec*ClpX	Hexamer*	3HWS	ADP	A	D184	5.3^{β}	R307	9.3^{α}	11.5 (D184-R307)
	*ec*HslU	Hexamer	1DO2	AMP-PNP	A	D256	4.9^{γ}	R325	9.4^{α}	12.7 (D256-R325)
	*ec*HslU	Hexamer	1HQY	ADP	E	D256	5.1^{β}	R325	9.5^{α}	14.0 (D256-R325)
	*ec*HslU	Hexamer	1G3I	ATP	A	D257	3.0^{γ}	R326	9.4^{α}	12.7 (D257-R326)
	*to*Lon	Hexamer	3K1J	ADP	B	D245	4.4^{β}	R311	6.8^{α}	10.3 (D245-R311)
PACTT core group	*st*ZraR	Hexamer	1OJL	ATP	E	D240	3.7^{γ}	R301	7.3^{α}	13.7 (E241-R301)
	*aa*NtrC1	Heptamer	3M0E	ATP	A	D238	5.2^{γ}	R299	2.9^{γ}	5.8 (D238-R299)
HEC group/DnaA Orc CDC6 clade	*hs*RuvB	Hexamer	2C9O	ADP	C	D302	4.9^{β}	R357	9.7^{α}	10.1 (D302-R357)
HEC group/clamp loader clade	*ec*Clamp loader	Pentamer	3GLF	ADP-BeF3	B	E127	4.8^{β}	R169	5.0^{β}	3.8 (E127-R169)
Helicase superfamily III	SV40 LTag helicase	Hexamer	1SVM	ATP	F	D474	3.4^{γ}	R540	3.1^{γ}	3.1 (D474-R540)
	*bp*E1	Hexamer	2V9P	None**	A	D479	3.1^{γ}	R538	3.0^{γ}	3.5 (D479-R538)

5. Protomer interaction in AAA+ hexamers

Most AAA+ proteins only show significant basal ATPase activity when two or more subunits are conjoined. In order to perform mechanical work they are typically organised in a higher oligomeric state (pentamer/hexamer/heptamer) and thread the substrate through the central pore of the ring. Since each ATPase module spends parts of its ATPase cycle disengaged from the substrate, protomer movements need to be coordinated for processive actions such as protein unfolding. Detailed knowledge about the mechano-chemical mechanisms involved in force generation is still missing. However, an indication of intersubunit communication arises from HslU and ClpX crystal structures, in which the C-terminal domains move relative to the ASCE domain during the ATPase cycle, changing the protomer interface according to the nucleotide binding state [36,64]. Despite lacking high resolution information, Hsp104 hexamers trapped in different nucleotide binding states also indicate substantial domain movements upon ATP binding and hydrolysis [65]. Moreover our asymmetric cryo EM reconstruction of Hsp104 in the same study shows changing protomer interfaces in the ring with deviation from the perfect six-fold symmetry. These data suggest that Hsp104 hexamers do not undergo concerted conformational change, but that only few protomers at a time move. In contrast, conformational change in the SV 40 LTag helicase hexamer [50] is thought to be concerted. In both examples, the subunits have to maintain interactions in any state in order to ensure hexamer stability. Given that many ATPases show salt sensitive oligomerisation, the most likely type of interaction ensuring oligomer formation would be salt bridges. Fig. 4 shows putative salt bridges between Ras and p120GAP and between nucleotide binding domains of the SV40 LTag helicase, p97 D1, p97 D2, HslU and RuvB as seen in oligomeric crystal structures.

The p120GAP encloses Ras on one side and creates a large interaction surface with three putative salt bridges between the proteins (Fig. 4A). The arginine finger is part of a sizable interaction area on p120GAP that contacts the nucleotide. None of the AAA+ structures displayed has similarly extended contacts with the nucleotide in the neighbouring subunit. One arginine finger residue of p97 D1, both of p97 D2 and the one in HslU are not participating in subunit contacts at all (Fig. 4C, D and E).

The SV40 LTag helicase crystal structure shows that protomer interactions are not restricted to the ASCE domain, but include the adjacent N-terminal domain. In fact, hexamerisation studies on the isolated ASCE domain confirm that the N-terminal domain is necessary for oligomerisation [66]. In most AAA+ proteins the ASCE domain is connected to additional N- or C-terminal domains, although few of the associated domains are implicated with hexamerisation but are rather linked to substrate recognition. An exception is the 40 residue C-terminal extension in Hsp104, which is involved in hexamerisation [67].

As mentioned before, p97 D1 is thought to promote oligomerisation in the AAA+ complex. Accordingly, the protomer interaction area in the p97 D1 domain is larger than in D2 and includes more putative salt bridges (Fig. 4C and D). Whilst the nucleotide and adjacent protomer show very small surface contacts in the p97 D1 domain, they have no interaction at all in p97 D2. The C-terminal domains in p97 contribute large interaction surfaces and could account for protomer communication in the rings. This mechanism of communication was first suggested for HslU [64] and it is therefore not surprising that the surface contacts in HslU are largely maintained by the C-terminal domain (Fig. 4E).

Of all depicted AAA+ proteins RuvB protomers show the biggest surface interaction area within the AAA+ domain. The contacts are surrounding the nucleotide binding pocket so tight that it would be impossible to exchange the bound ADP in the hexameric assembly [68]. Accordingly, purified human RuvB only shows marginal ATPase and no helicase activity and it was speculated that co-factors are necessary to obtain full enzymatic activity [68–70].

6. Concluding remarks

Over the past 20 years, phylogenetic, structural and functional analysis of AAA+ ATPases has advanced our knowledge about members of this superfamily enormously. With our growing understanding about the structure and function of single AAA+ proteins the question arises

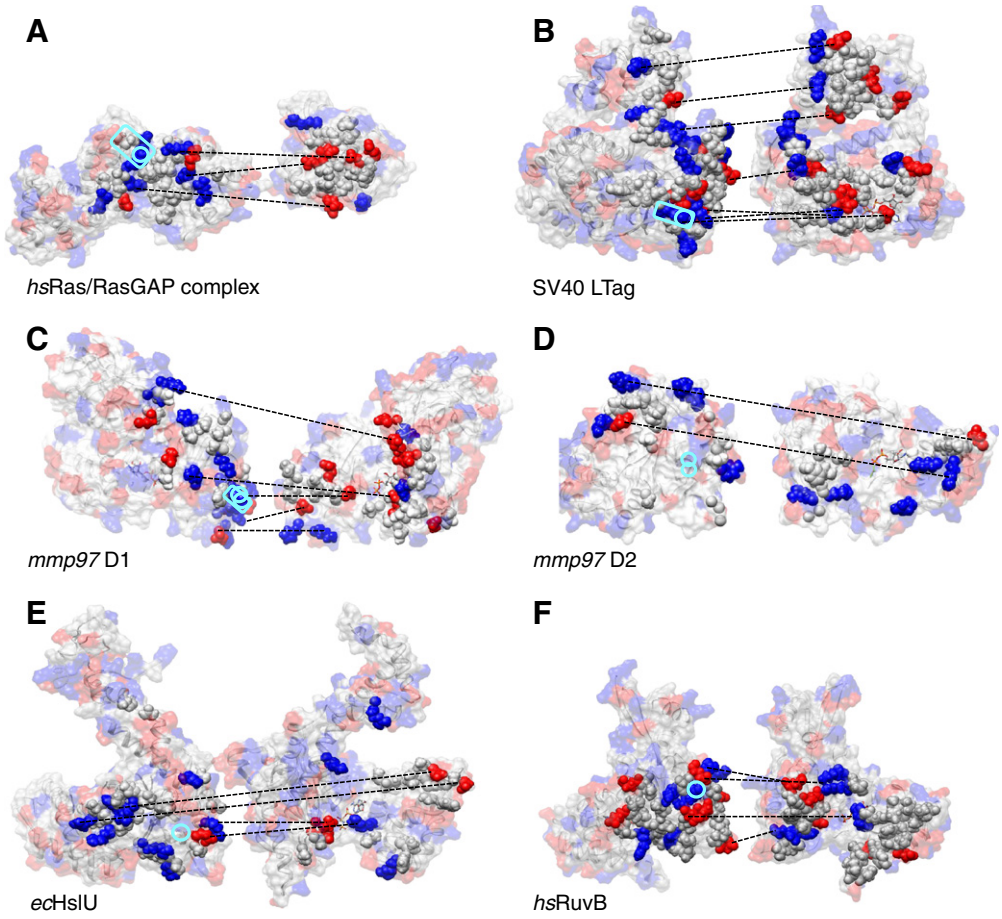

Fig. 4. Subunit interfaces of Ras/p120GAP and selected ASCE ATPases. Surface representations of the opened out subunit interfaces of *hs*Ras and p120GAP (A) and hexameric structures of SV40 LTag helicase (B), *mm*p97 D1 (C), *mm*p97 D2 (D), *ec*HslU (E) and *hs*RuvB (F) are shown. The same PDB structures as in Fig. 3 were used. MSMS surfaces of all proteins are coloured in transparent grey. Charged residues are coloured transparent red (Asp, Glu) or blue (Arg, His, Lys). An inter-atomic distance d ≤ 0.4 Å + van-der-Waals radius 1 + van-der-Waals radius 2 was taken as a contact criterion. Residues contacting amino acids, nucleotide or structural water of the adjacent subunit in the hexamer are depicted as a sphere in bold colours. Putative salt bridges between adjacent subunits are indicated. The position of arginine fingers and areas in contact with the nucleotide of the adjacent subunit are highlighted as a cyan circle and rectangles, respectively. All calculation and structure manipulations were performed using UCSF Chimera.

how these proteins compare to each other. Striking similarities of all AAA+ ATPases are the strong structural conservation of the ASCE domain and its hexameric arrangement in the active complex. However, there are exceptions to the rule. Some AAA+ proteins lack characteristic motifs such as the sensor 1, sensor 2 or arginine finger or display aberrant oligomerisation properties (Table 2). It is often difficult to pinpoint the specific structural reason for a functional difference and *vice versa*. For the similar task of feeding polypeptide chains into the proteolytic chamber of ClpP a single (ClpX) and a tandem (ClpA) ASCE domain protein evolved, arguing that there must be important operational differences between these proteins. Another exception is p97, which is thought to be involved in extraction and endoplasmatic reticulum associated degradation (ERAD) of misfolded proteins. Unlike other double tiered proteins with similar tasks (e.g. ClpB or ClpA), which translocate their substrates through the central pore of the hexamer, p97 does not pass substrates through the D1 ring [71]. Thus, given how diverse the tasks of proteins of the AAA+ superfamily are it might not be possible to develop a unifying operative model for all ATPases despite obvious structural similarities.

Moreover, it is likely that small structural variations in the AAA+ domain contribute to the diversification and specialisation seen in this heterogeneous superfamily. Different AAA+ families present structural characteristics that have not been correlated to functional effects in all cases to date. Taking the arginine finger as an example, it is obvious from our comparison of nucleotide binding pockets (Fig. 3), that the basic residues can be arranged in multiple ways to aid nucleotide hydrolysis. However, it is not clear, why some ATPases have only one arginine finger residue, whilst others have two consecutive or two spaced-out arginine fingers. In addition, the structural and functional data indicate that the sensor 2 arginine could adopt an arginine-finger-like function and participate in ATP hydrolysis. In combination with the finding that the C-terminal domain which harbours the sensor 2 residue can move relative to the ASCE domain [36,64] this notion is particularly intriguing. Our structural comparison however is constrained by the available crystal structures, which frequently have ADP rather than ATP bound to the binding pocket. In particular sensor 2 containing AAA+ ATPases rarely form hexamers in crystals and those structures which could be resolved in the oligomeric state often show the arginine finger rotated away from the nucleotide. Taken together, the functional role of these basic residues might differ subtly between the different clades adding to the functional variety of AAA+ ATPases.

There are also numerous alternative oligomeric assembly models that do not conform to the classical hexameric ATPase packing as seen in many crystal structures. Based on cryo EM reconstructions of Hsp104 and supporting biochemical data we suggested an atypical hexameric packing where the coiled-coil insertion in Hsp104 D1 intercalates between the ATPase domains and possibly provides an arginine residue to the nucleotide binding pocket [72]. As another example, crystal structures of the BchI Mg chelatase and MoxR

families display an unusual spatial arrangement of the C-terminal domain (PBD ID: 1G8P, 3NBX). In the hexameric models the C-terminal domain of one domain comes to lie in close proximity to the nucleotide in the ASCE domain of the neighbouring subunit allowing for the sensor 2 residue to act in *trans* [73]. Furthermore the crystal structure of the CED-4 apoptosome shows an octameric assembly with an atypical interface between protomers, separating this evolutionary more distant group of STAND proteins also structurally from the AAA+ ATPases discussed in this review [74]. Yet, pentameric clamp loaders and heptameric NtrC1 assemblies also deviate from the hexameric arrangement.

Many AAA+ ATPases are thought to couple ATP turnover with substrate binding and/or translocation through the central pore, but the mechanistic details of this interaction still remain unclear. Single molecule studies on the pentameric Φ29 DNA packaging motor and single chain ClpXΔN variants reveal that these motors can perform significant mechanical work threading substrate through the central pore against loads as high as 57 and 20 pN, respectively [75–77]. Interestingly, subunits in both proteins take step sizes of 8.5–10 Å, even though the properties of the DNA and protein substrates differ considerably. These data are particularly useful when movements of substrate interacting loops or domains are examined on a structural level. They also indicate that there must be a certain degree of co-operativity between protomers in order to process the substrate in a linear fashion. However, for many protein-interacting AAA+ ATPases assessment of motor efficiency is a challenging task. To begin with, their substrates are often aggregated polypeptides and/or membrane bound proteins and secondly some proteins (e.g. ClpB) exchange protomers in the functional complex on a second timescale [78,79].

In order to advance our understanding about the subtle differences between AAA+ proteins and their functional specifications all possible information on the different dynamic states of these flexible molecular motors should be taken into consideration. In particular molecular snapshots of substrate bound structures could provide valuable insight into the mechanochemical coupling between ATP hydrolysis and substrate processing. The central position of many AAA+ assemblies in essential cellular pathways makes them a fascinating subject of research at present and in the future.

Acknowledgments

We thank Helen Saibil, Marta Carroni and James Shorter for critical comments on the manuscript. All authors are funded by the DFG Emmy Noether Program (WE 4628/1-1 to PW).

References

[1] F.J. Kull, R.D. Vale, R.J. Fletterick, The case for a common ancestor: kinesin and myosin motor proteins and G proteins, J. Muscle Res. Cell Motil. 19 (1998) 877–886.
[2] R.D. Vale, R.A. Milligan, The way things move: looking under the hood of molecular motor proteins, Science 288 (2000) 88–95.
[3] M.R. Singleton, D.B. Wigley, Modularity and specialization in superfamily 1 and 2 helicases, J. Bacteriol. 184 (2002) 1819–1826.
[4] M.S. Dillingham, Superfamily I helicases as modular components of DNA-processing machines, Biochem. Soc. Trans. 39 (2011) 413–423.
[5] M. Dean, T. Annilo, Evolution of the ATP-binding cassette (ABC) transporter superfamily in vertebrates, Annu. Rev. Genomics Hum. Genet. 6 (2005) 123–142.
[6] A.P. Carter, C. Cho, L. Jin, R.D. Vale, Crystal structure of the dynein motor domain, Science 331 (2011) 1159–1165.
[7] C. Ulbrich, M. Diepholz, J. Bassler, D. Kressler, B. Pertschy, K. Galani, B. Bottcher, E. Hurt, Mechanochemical removal of ribosome biogenesis factors from nascent 60S ribosomal subunits, Cell 138 (2009) 911–922.
[8] K.R. Simonetta, S.L. Kazmirski, E.R. Goedken, A.J. Cantor, B.A. Kelch, R. McNally, S. N. Seyedin, D.L. Makino, M. O'Donnell, J. Kuriyan, The mechanism of ATP-dependent primer-template recognition by a clamp loader complex, Cell 137 (2009) 659–671.
[9] R. Erdmann, F.F. Wiebel, A. Flessau, J. Rytka, A. Beyer, K.U. Frohlich, W.H. Kunau, PAS1, a yeast gene required for peroxisome biogenesis, encodes a member of a novel family of putative ATPases, Cell 64 (1991) 499–510.
[10] S.Y. Lee, A. De La Torre, D. Yan, S. Kustu, B.T. Nixon, D.E. Wemmer, Regulation of the transcriptional activator NtrC1: structural studies of the regulatory and AAA+ ATPase domains, Genes Dev. 17 (2003) 2552–2563.
[11] L.M. Iyer, D.D. Leipe, E.V. Koonin, L. Aravind, Evolutionary history and higher order classification of AAA+ ATPases, J. Struct. Biol. 146 (2004) 11–31.
[12] J.P. Erzberger, J.M. Berger, Evolutionary relationships and structural mechanisms of AAA+ proteins, Annu. Rev. Biophys. Biomol. Struct. 35 (2006) 93–114.
[13] M. Ammelburg, T. Frickey, A.N. Lupas, Classification of AAA+ proteins, J. Struct. Biol. 156 (2006) 2–11.
[14] J. Gough, K. Karplus, R. Hughey, C. Chothia, Assignment of homology to genome sequences using a library of hidden Markov models that represent all proteins of known structure, J. Mol. Biol. 313 (2001) 903–919.
[15] J.E. Walker, M. Saraste, M.J. Runswick, N.J. Gay, Distantly related sequences in the alpha- and beta-subunits of ATP synthase, myosin, kinases and other ATP-requiring enzymes and a common nucleotide binding fold, EMBO J. 1 (1982) 945–951.
[16] X. Zhang, D.B. Wigley, The 'glutamate switch' provides a link between ATPase activity and ligand binding in AAA+ proteins, Nat. Struct. Mol. Biol. 15 (2008) 1223–1227.
[17] K. Scheffzek, M.R. Ahmadian, W. Kabsch, L. Wiesmuller, A. Lautwein, F. Schmitz, A. Wittinghofer, The Ras–RasGAP complex: structural basis for GTPase activation and its loss in oncogenic Ras mutants, Science 277 (1997) 333–338.
[18] K. Scheffzek, M.R. Ahmadian, GTPase activating proteins: structural and functional insights 18 years after discovery, Cell. Mol. Life Sci. 62 (2005) 3014–3038.
[19] I. Botos, E.E. Melnikov, S. Cherry, A.G. Khalatova, F.S. Rasulova, J.E. Tropea, M.R. Maurizi, T.V. Rotanova, A. Gustchina, A. Wlodawer, Crystal structure of the AAA+ alpha domain of *E. coli* Lon protease at 1.9 A resolution, J. Struct. Biol. 146 (2004) 113–122.
[20] M. Saraste, P.R. Sibbald, A. Wittinghofer, The P-loop—a common motif in ATP- and GTP-binding proteins, Trends Biochem. Sci. 15 (1990) 430–434.
[21] D.A. Hattendorf, S.L. Lindquist, Cooperative kinetics of both Hsp104 ATPase domains and interdomain communication revealed by AAA sensor-1 mutants, EMBO J. 21 (2002) 12–21.
[22] S. Schlee, Y. Groemping, P. Herde, R. Seidel, J. Reinstein, The chaperone function of ClpB from *Thermus thermophilus* depends on allosteric interactions of its two ATP-binding sites, J. Mol. Biol. 306 (2001) 889–899.
[23] S.W. Whiteheart, K. Rossnagel, S.A. Buhrow, M. Brunner, R. Jaenicke, J.E. Rothman, N-ethylmaleimide-sensitive fusion protein: a trimeric ATPase whose hydrolysis of ATP is required for membrane fusion, J. Cell Biol. 126 (1994) 945–954.
[24] F. Beuron, T.C. Flynn, J. Ma, H. Kondo, X. Zhang, P.S. Freemont, Motions and negative cooperativity between p97 domains revealed by cryo-electron microscopy and quantised elastic deformational model, J. Mol. Biol. 327 (2003) 619–629.
[25] S. Nishikori, M. Esaki, K. Yamanaka, S. Sugimoto, T. Ogura, Positive cooperativity of the p97 AAA ATPase is critical for essential functions, J. Biol. Chem. 286 (2011) 15815–15820.
[26] Q. Wang, C. Song, C.C. Li, Hexamerization of p97-VCP is promoted by ATP binding to the D1 domain and required for ATPase and biological activities, Biochem. Biophys. Res. Commun. 300 (2003) 253–260.
[27] B. DeLaBarre, A.T. Brunger, Complete structure of p97/valosin-containing protein reveals communication between nucleotide domains, Nat. Struct. Biol. 10 (2003) 856–863.
[28] W.K. Tang, D. Li, C.C. Li, L. Esser, R. Dai, L. Guo, D. Xia, A novel ATP-dependent conformation in p97 N-D1 fragment revealed by crystal structures of disease-related mutants, EMBO J. 29 (2010) 2217–2229.
[29] E.C. Schirmer, C. Queitsch, A.S. Kowal, D.A. Parsell, S. Lindquist, The ATPase activity of Hsp104, effects of environmental conditions and mutations, J. Biol. Chem. 273 (1998) 15546–15552.
[30] E.C. Schirmer, D.M. Ware, C. Queitsch, A.S. Kowal, S.L. Lindquist, Subunit interactions influence the biochemical and biological properties of Hsp104, Proc. Natl. Acad. Sci. U. S. A. 98 (2001) 914–919.
[31] B. Rockel, J. Jakana, W. Chiu, W. Baumeister, Electron cryo-microscopy of VAT, the archaeal p97/CDC48 homologue from *Thermoplasma acidophilum*, J. Mol. Biol. 317 (2002) 673–681.
[32] I. Dreveny, H. Kondo, K. Uchiyama, A. Shaw, X. Zhang, P.S. Freemont, Structural basis of the interaction between the AAA ATPase p97/VCP and its adaptor protein p47, EMBO J. 23 (2004) 1030–1039.
[33] G. Effantin, R. Rosenzweig, M.H. Glickman, A.C. Steven, Electron microscopic evidence in support of alpha-solenoid models of proteasomal subunits Rpn1 and Rpn2, J. Mol. Biol. 386 (2009) 1204–1211.
[34] J. Hinnerwisch, W.A. Fenton, K.J. Furtak, G.W. Farr, A.L. Horwich, Loops in the central channel of ClpA chaperone mediate protein binding, unfolding, and translocation, Cell 121 (2005) 1029–1041.
[35] G. Thibault, Y. Tsitrin, T. Davidson, A. Gribun, W.A. Houry, Large nucleotide-dependent movement of the N-terminal domain of the ClpX chaperone, EMBO J. 25 (2006) 3367–3376.
[36] S.E. Glynn, A. Martin, A.R. Nager, T.A. Baker, R.T. Sauer, Structures of asymmetric ClpX hexamers reveal nucleotide-dependent motions in a AAA+ protein-unfolding machine, Cell 139 (2009) 744–756.
[37] F. Wang, Z. Mei, Y. Qi, C. Yan, Q. Hu, J. Wang, Y. Shi, Structure and mechanism of the hexameric MecA-ClpC molecular machine, Nature 471 (2011) 331–335.
[38] C. Zhao, E.A. Matveeva, Q. Ren, S.W. Whiteheart, Dissecting the N-ethylmaleimide-sensitive factor: required elements of the N and D1 domains, J. Biol. Chem. 285 (2010) 761–772.
[39] J. Furst, R.B. Sutton, J. Chen, A.T. Brunger, N. Grigorieff, Electron cryomicroscopy structure of N-ethyl maleimide sensitive factor at 11 A resolution, EMBO J. 22 (2003) 4365–4374.

[40] M. Babst, B. Wendland, E.J. Estepa, S.D. Emr, The Vps4p AAA ATPase regulates membrane association of a Vps protein complex required for normal endosome function, EMBO J. 17 (1998) 2982–2993.
[41] A. Scott, H.Y. Chung, M. Gonciarz-Swiatek, G.C. Hill, F.G. Whitby, J. Gaspar, J. M. Holton, R. Viswanathan, S. Ghaffarian, C.P. Hill, W.I. Sundquist, Structural and mechanistic studies of VPS4 proteins, EMBO J. 24 (2005) 3658–3669.
[42] R.M. Story, T.A. Steitz, Structure of the recA protein–ADP complex, Nature 355 (1992) 374–376.
[43] W. Kress, H. Mutschler, E. Weber-Ban, Both ATPase domains of ClpA are critical for processing of stable protein structures, J. Biol. Chem. 284 (2009) 31441–31452.
[44] A. Gerega, B. Rockel, J. Peters, T. Tamura, W. Baumeister, P. Zwickl, VAT, the thermoplasma homolog of mammalian p97/VCP, is an N domain-regulated protein unfoldase, J. Biol. Chem. 280 (2005) 42856–42862.
[45] A. Schaupp, M. Marcinowski, V. Grimminger, B. Bosl, S. Walter, Processing of proteins by the molecular chaperone Hsp104, J. Mol. Biol. 370 (2007) 674–686.
[46] Y.H. Watanabe, K. Motohashi, M. Yoshida, Roles of the two ATP binding sites of ClpB from *Thermus thermophilus*, J. Biol. Chem. 277 (2002) 5804–5809.
[47] A. Mogk, C. Schlieker, C. Strub, W. Rist, J. Weibezahn, B. Bukau, Roles of individual domains and conserved motifs of the AAA+ chaperone ClpB in oligomerization, ATP hydrolysis, and chaperone activity, J. Biol. Chem. 278 (2003) 17615–17624.
[48] S.M. Doyle, J. Shorter, M. Zolkiewski, J.R. Hoskins, S. Lindquist, S. Wickner, Asymmetric deceleration of ClpB or Hsp104 ATPase activity unleashes protein-remodeling activity, Nat. Struct. Mol. Biol. 14 (2007) 114–122.
[49] C.U. Lenzen, D. Steinmann, S.W. Whiteheart, W.I. Weis, Crystal structure of the hexamerization domain of N-ethylmaleimide-sensitive fusion protein, Cell 94 (1998) 525–536.
[50] D. Gai, R. Zhao, D. Li, C.V. Finkielstein, X.S. Chen, Mechanisms of conformational change for a replicative hexameric helicase of SV40 large tumor antigen, Cell 119 (2004) 47–60.
[51] B. Chen, T.A. Sysoeva, S. Chowdhury, L. Guo, S. De Carlo, J.A. Hanson, H. Yang, B.T. Nixon, Engagement of arginine finger to ATP triggers large conformational changes in NtrC1 AAA+ ATPase for remodeling bacterial RNA polymerase, Structure 18 (2010) 1420–1430.
[52] B. Guenther, R. Onrust, A. Sali, M. O'Donnell, J. Kuriyan, Crystal structure of the delta' subunit of the clamp-loader complex of *E. coli* DNA polymerase III, Cell 91 (1997) 335–345.
[53] J.M. Davies, A.T. Brunger, W.I. Weis, Improved structures of full-length p97, an AAA ATPase: implications for mechanisms of nucleotide-dependent conformational change, Structure 16 (2008) 715–726.
[54] A.F. Neuwald, L. Aravind, J.L. Spouge, E.V. Koonin, AAA+: A class of chaperone-like ATPases associated with the assembly, operation, and disassembly of protein complexes, Genome Res. 9 (1999) 27–43.
[55] C.W. Muller, G.E. Schulz, Structure of the complex between adenylate kinase from *Escherichia coli* and the inhibitor Ap5A refined at 1.9 A resolution. A model for a catalytic transition state, J. Mol. Biol. 224 (1992) 159–177.
[56] T. Ogura, S.W. Whiteheart, A.J. Wilkinson, Conserved arginine residues implicated in ATP hydrolysis, nucleotide-sensing, and inter-subunit interactions in AAA and AAA+ ATPases, J. Struct. Biol. 146 (2004) 106–112.
[57] S.A. Joshi, G.L. Hersch, T.A. Baker, R.T. Sauer, Communication between ClpX and ClpP during substrate processing and degradation, Nat. Struct. Mol. Biol. 11 (2004) 404–411.
[58] K. Karata, T. Inagawa, A.J. Wilkinson, T. Tatsuta, T. Ogura, Dissecting the role of a conserved motif (the second region of homology) in the AAA family of ATPases. Site-directed mutagenesis of the ATP-dependent protease FtsH, J. Biol. Chem. 274 (1999) 26225–26232.
[59] Q. Wang, C. Song, L. Irizarry, R. Dai, X. Zhang, C.C. Li, Multifunctional roles of the conserved Arg residues in the second region of homology of p97/valosin-containing protein, J. Biol. Chem. 280 (2005) 40515–40523.
[60] C.D. Putnam, S.B. Clancy, H. Tsuruta, S. Gonzalez, J.G. Wetmur, J.A. Tainer, Structure and mechanism of the RuvB Holliday junction branch migration motor, J. Mol. Biol. 311 (2001) 297–310.
[61] I. Rombel, P. Peters-Wendisch, A. Mesecar, T. Thorgeirsson, Y.K. Shin, S. Kustu, MgATP binding and hydrolysis determinants of NtrC, a bacterial enhancer-binding protein, J. Bacteriol. 181 (1999) 4628–4638.
[62] N.D. Werbeck, J.N. Kellner, T.R. Barends, J. Reinstein, Nucleotide binding and allosteric modulation of the second AAA+ domain of ClpB probed by transient kinetic studies, Biochemistry 48 (2009) 7240–7250.
[63] M. Esaki, T. Ogura, ATP-bound form of the D1 AAA domain inhibits an essential function of Cdc48p/p97, Biochem. Cell Biol. 88 (2010) 109–117.
[64] J. Wang, J.J. Song, M.C. Franklin, S. Kamtekar, Y.J. Im, S.H. Rho, I.S. Seong, C.S. Lee, C.H. Chung, S.H. Eom, Crystal structures of the HslVU peptidase–ATPase complex reveal an ATP-dependent proteolysis mechanism, Structure 9 (2001) 177–184.
[65] P. Wendler, J. Shorter, D. Snead, C. Plisson, D.K. Clare, S. Lindquist, H.R. Saibil, Motor mechanism for protein threading through Hsp104, Mol. Cell 34 (2009) 81–92.
[66] D. Li, R. Zhao, W. Lilyestrom, D. Gai, R. Zhang, J.A. DeCaprio, E. Fanning, A. Jochimiak, G. Szakonyi, X.S. Chen, Structure of the replicative helicase of the oncoprotein SV40 large tumour antigen, Nature 423 (2003) 512–518.
[67] R.G. Mackay, C.W. Helsen, J.M. Tkach, J.R. Glover, The C-terminal extension of *Saccharomyces cerevisiae* Hsp104 plays a role in oligomer assembly, Biochemistry 47 (2008) 1918–1927.
[68] P.M. Matias, S. Gorynia, P. Donner, M.A. Carrondo, Crystal structure of the human AAA+ protein RuvBL1, J. Biol. Chem. 281 (2006) 38918–38929.
[69] T. Puri, P. Wendler, B. Sigala, H. Saibil, I.R. Tsaneva, Dodecameric structure and ATPase activity of the human TIP48/TIP49 complex, J. Mol. Biol. 366 (2007) 179–192.
[70] T. Ikura, V.V. Ogryzko, M. Grigoriev, R. Groisman, J. Wang, M. Horikoshi, R. Scully, J. Qin, Y. Nakatani, Involvement of the TIP60 histone acetylase complex in DNA repair and apoptosis, Cell 102 (2000) 463–473.
[71] B. DeLaBarre, J.C. Christianson, R.R. Kopito, A.T. Brunger, Central pore residues mediate the p97/VCP activity required for ERAD, Mol. Cell 22 (2006) 451–462.
[72] P. Wendler, J. Shorter, C. Plisson, A.G. Cashikar, S. Lindquist, H.R. Saibil, Atypical AAA+ subunit packing creates an expanded cavity for disaggregation by the protein-remodeling factor Hsp104, Cell 131 (2007) 1366–1377.
[73] M.J. Moreau, A.T. McGeoch, A.R. Lowe, L.S. Itzhaki, S.D. Bell, ATPase site architecture and helicase mechanism of an archaeal MCM, Mol. Cell 28 (2007) 304–314.
[74] S. Qi, Y. Pang, Q. Hu, Q. Liu, H. Li, Y. Zhou, T. He, Q. Liang, Y. Liu, X. Yuan, G. Luo, J. Wang, N. Yan, Y. Shi, Crystal structure of the *Caenorhabditis elegans* apoptosome reveals an octameric assembly of CED-4, Cell 141 (2010) 446–457.
[75] J.R. Moffitt, Y.R. Chemla, K. Aathavan, S. Grimes, P.J. Jardine, D.L. Anderson, C. Bustamante, Intersubunit coordination in a homomeric ring ATPase, Nature 457 (2009) 446–450.
[76] R.A. Maillard, G. Chistol, M. Sen, M. Righini, J. Tan, C.M. Kaiser, C. Hodges, A. Martin, C. Bustamante, ClpX(P) generates mechanical force to unfold and translocate its protein substrates, Cell 145 (2011) 459–469.
[77] M.E. Aubin-Tam, A.O. Olivares, R.T. Sauer, T.A. Baker, M.J. Lang, Single-molecule protein unfolding and translocation by an ATP-fueled proteolytic machine, Cell 145 (2011) 257–267.
[78] T. Haslberger, A. Zdanowicz, I. Brand, J. Kirstein, K. Turgay, A. Mogk, B. Bukau, Protein disaggregation by the AAA+ chaperone ClpB involves partial threading of looped polypeptide segments, Nat. Struct. Mol. Biol. 15 (2008) 641–650.
[79] N.D. Werbeck, S. Schlee, J. Reinstein, Coupling and dynamics of subunits in the hexameric AAA+ chaperone ClpB, J. Mol. Biol. 378 (2008) 178–190.
[80] E.F. Pettersen, T.D. Goddard, C.C. Huang, G.S. Couch, D.M. Greenblatt, E.C. Meng, T.E. Ferrin, UCSF Chimera — a visualization system for exploratory research and analysis, J. Comput. Chem. 25 (2004) 1605–1612.
[81] S.K. Singh, M.R. Maurizi, Mutational analysis demonstrates different functional roles for the two ATP-binding sites in ClpAP protease from *Escherichia coli*, J. Biol. Chem. 269 (1994) 29537–29545.
[82] H. Iwasaki, Y.W. Han, T. Okamoto, T. Ohnishi, M. Yoshikawa, K. Yamada, H. Toh, H. Daiyasu, T. Ogura, H. Shinagawa, Mutational analysis of the functional motifs of RuvB, an AAA+ class helicase and motor protein for holliday junction branch migration, Mol. Microbiol. 36 (2000) 528–538.
[83] M. Babst, T.K. Sato, L.M. Banta, S.D. Emr, Endosomal transport function in yeast requires a novel AAA-type ATPase, Vps4p, EMBO J. 16 (1997) 1820–1831.
[84] B.A. Davies, I.F. Azmi, J. Payne, A. Shestakova, B.F. Horazdovsky, M. Babst, D.J. Katzmann, Coordination of substrate binding and ATP hydrolysis in Vps4-mediated ESCRT-III disassembly, Mol. Biol. Cell. 21 (2010) 3396–3408.
[85] N. Bishop, P. Woodman, ATPase-defective mammalian VPS4 localizes to aberrant endosomes and impairs cholesterol trafficking, Mol. Biol. Cell 11 (2000) 227–239.
[86] H. Huang, K. Zhao, D.R. Arnett, E. Fanning, A specific docking site for DNA polymerase {alpha}-primase on the SV40 helicase is required for viral primosome activity, but helicase activity is dispensable, J. Biol. Chem. 285 (2010) 33475–33484.
[87] W.B. Greenleaf, J. Shen, D. Gai, X.S. Chen, Systematic study of the functions for the residues around the nucleotide pocket in simian virus 40 AAA+ hexameric helicase, J. Virol. 82 (2008) 6017–6023.
[88] B.M. Weiner, M.K. Bradley, Specific mutation of a regulatory site within the ATP-binding region of simian virus 40 large T antigen, J. Virol. 65 (1991) 4973–4984.
[89] K.I. Kim, G.W. Cheong, S.C. Park, J.S. Ha, K.M. Woo, S.J. Choi, C.H. Chung, Heptameric ring structure of the heat-shock protein ClpB, a protein-activated ATPase in *Escherichia coli*, J. Mol. Biol. 303 (2000) 655–666.
[90] A.M. Castellino, P. Cantalupo, I.M. Marks, J.V. Vartikar, K.W. Peden, J.M. Pipas, trans-Dominant and non-trans-dominant mutant simian virus 40 large T antigens show distinct responses to ATP, J. Virol. 71 (1997) 7549–7559.
[91] J.M. Farber, K.W. Peden, D. Nathans, trans-Dominant defective mutants of simian virus 40 T antigen, J. Virol. 61 (1987) 436–445.
[92] H. Besche, N. Tamura, T. Tamura, P. Zwickl, Mutational analysis of conserved AAA + residues in the archaeal Lon protease from *Thermoplasma acidophilum*, FEBS Lett. 574 (2004) 161–166.
[93] D.S. Weiss, J. Batut, K.E. Klose, J. Keener, S. Kustu, The phosphorylated form of the enhancer-binding protein NTRC has an ATPase activity that is essential for activation of transcription, Cell 67 (1991) 155–167.
[94] G. Perkins, J.F. Diffley, Nucleotide-dependent prereplicative complex assembly by Cdc6p, a homolog of eukaryotic and prokaryotic clamp-loaders, Mol. Cell 2 (1998) 23–32.
[95] K.I. Kim, K.M. Woo, I.S. Seong, Z.W. Lee, S.H. Baek, C.H. Chung, Mutational analysis of the two ATP-binding sites in ClpB, a heat shock protein with protein-activated ATPase activity in *Escherichia coli*, Biochem. J. 333 (Pt 3) (1998) 671–676.
[96] M.R. Ahmadian, T. Zor, D. Vogt, W. Kabsch, Z. Selinger, A. Wittinghofer, K. Scheffzek, Guanosine triphosphatase stimulation of oncogenic Ras mutants, Proc. Natl. Acad. Sci. U. S. A. 96 (1999) 7065–7070.
[97] M. Weinreich, C. Liang, B. Stillman, The Cdc6p nucleotide-binding motif is required for loading mcm proteins onto chromatin, Proc. Natl. Acad. Sci. U. S. A. 96 (1999) 441–446.

[98] A.K. North, D.S. Weiss, H. Suzuki, Y. Flashner, S. Kustu, Repressor forms of the enhancer-binding protein NrtC: some fail in coupling ATP hydrolysis to open complex formation by sigma 54-holoenzyme, J. Mol. Biol. 260 (1996) 317–331.
[99] A. Seybert, D.B. Wigley, Distinct roles for ATP binding and hydrolysis at individual subunits of an archaeal clamp loader, EMBO J. 23 (2004) 1360–1371.
[100] F. Zhang, Z. Wu, P. Zhang, G. Tian, D. Finley, Y. Shi, Mechanism of substrate unfolding and translocation by the regulatory particle of the proteasome from *Methanocaldococcus jannaschii*, Mol. Cell 34 (2009) 485–496.
[101] A. Schepers, J.F. Diffley, Mutational analysis of conserved sequence motifs in the budding yeast Cdc6 protein, J. Mol. Biol. 308 (2001) 597–608.
[102] B. Wang, L. Feng, Y. Hu, S.H. Huang, C.P. Reynolds, L. Wu, A.Y. Jong, The essential role of *Saccharomyces cerevisiae* CDC6 nucleotide-binding site in cell growth, DNA synthesis, and Orc1 association, J. Biol. Chem. 274 (1999) 8291–8298.
[103] A.A. Horwitz, A. Navon, M. Groll, D.M. Smith, C. Reis, A.L. Goldberg, ATP-induced structural transitions in PAN, the proteasome-regulatory ATPase complex in Archaea, J. Biol. Chem. 282 (2007) 22921–22929.
[104] N. Takahashi, S. Tsutsumi, T. Tsuchiya, B. Stillman, T. Mizushima, Functions of sensor 1 and sensor 2 regions of *Saccharomyces cerevisiae* Cdc6p in vivo and in vitro, J. Biol. Chem. 277 (2002) 16033–16040.
[105] J. Cai, N. Yao, E. Gibbs, J. Finkelstein, B. Phillips, M. O'Donnell, J. Hurwitz, ATP hydrolysis catalyzed by human replication factor C requires participation of multiple subunits, Proc. Natl. Acad. Sci. U. S. A. 95 (1998) 11607–11612.
[106] K. Turgay, M. Persuh, J. Hahn, D. Dubnau, Roles of the two ClpC ATP binding sites in the regulation of competence and the stress response, Mol. Microbiol. 42 (2001) 717–727.
[107] B. Bosl, V. Grimminger, S. Walter, Substrate binding to the molecular chaperone Hsp104 and its regulation by nucleotides, J. Biol. Chem. 280 (2005) 38170–38176.
[108] D.A. Parsell, A.S. Kowal, M.A. Singer, S. Lindquist, Protein disaggregation mediated by heat-shock protein Hsp104, Nature 372 (1994) 475–478.
[109] D.A. Parsell, A.S. Kowal, S. Lindquist, *Saccharomyces cerevisiae* Hsp104 protein. Purification and characterization of ATP-induced structural changes, J. Biol. Chem. 269 (1994) 4480–4487.
[110] J.M. Tkach, J.R. Glover, Amino acid substitutions in the C-terminal AAA+ module of Hsp104 prevent substrate recognition by disrupting oligomerization and cause high temperature inactivation, J. Biol. Chem. 279 (2004) 35692–35701.
[111] J. Krzewska, G. Konopa, K. Liberek, Importance of two ATP-binding sites for oligomerization, ATPase activity and chaperone function of mitochondrial Hsp78 protein, J. Mol. Biol. 314 (2001) 901–910.
[112] H.K. Song, C. Hartmann, R. Ramachandran, M. Bochtler, R. Behrendt, L. Moroder, R. Huber, Mutational studies on HslU and its docking mode with HslV, Proc. Natl. Acad. Sci. U. S. A. 97 (2000) 14103–14108.
[113] L.C. Briggs, G.S. Baldwin, N. Miyata, H. Kondo, X. Zhang, P.S. Freemont, Analysis of nucleotide binding to P97 reveals the properties of a tandem AAA hexameric ATPase, J. Biol. Chem. 283 (2008) 13745–13752.
[114] G.L. Hersch, R.E. Burton, D.N. Bolon, T.A. Baker, R.T. Sauer, Asymmetric interactions of ATP with the AAA+ ClpX6 unfoldase: allosteric control of a protein machine, Cell 121 (2005) 1017–1027.
[115] E.A. Matveeva, A.P. May, P. He, S.W. Whiteheart, Uncoupling the ATPase activity of the N-ethylmaleimide sensitive factor (NSF) from 20S complex disassembly, Biochemistry 41 (2002) 530–536.
[116] C. Song, Q. Wang, C.C. Li, ATPase activity of p97-valosin-containing protein (VCP). D2 mediates the major enzyme activity, and D1 contributes to the heat-induced activity, J. Biol. Chem. 278 (2003) 3648–3655.
[117] G.D. Bowman, M. O'Donnell, J. Kuriyan, Structural analysis of a eukaryotic sliding DNA clamp-clamp loader complex, Nature 429 (2004) 724–730.
[118] Y. Akiyama, A. Kihara, H. Tokuda, K. Ito, FtsH (HflB) is an ATP-dependent protease selectively acting on SecY and some other membrane proteins, J. Biol. Chem. 271 (1996) 31196–31201.
[119] D.A. Hattendorf, S.L. Lindquist, Analysis of the AAA sensor-2 motif in the C-terminal ATPase domain of Hsp104 with a site-specific fluorescent probe of nucleotide binding, Proc. Natl. Acad. Sci. U. S. A. 99 (2002) 2732–2737.
[120] D.H. Shin, S.J. Yoo, Y.K. Shim, J.H. Seol, M.S. Kang, C.H. Chung, Mutational analysis of the ATP-binding site in HslU, the ATPase component of HslVU protease in *Escherichia coli*, FEBS Lett. 398 (1996) 151–154.
[121] T. Hishida, H. Iwasaki, T. Yagi, H. Shinagawa, Role of walker motif A of RuvB protein in promoting branch migration of holliday junctions. Walker motif a mutations affect Atp binding, Atp hydrolyzing, and DNA binding activities of Ruvb, J. Biol. Chem. 274 (1999) 25335–25342.
[122] A. Johnson, M. O'Donnell, Ordered ATP hydrolysis in the gamma complex clamp loader AAA+ machine, J. Biol. Chem. 278 (2003) 14406–14413.